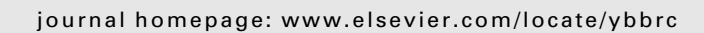
ELSEVIER

Contents lists available at ScienceDirect

# Biochemical and Biophysical Research Communications





# A novel sorting strategy of trichosanthin for hijacking human immunodeficiency virus type 1

Wen-Long Zhao, Fan Zhang, Du Feng, Ju Wu, Shan Chen, Sen-Fang Sui \*

Department of Biological Sciences and Biotechnology, State Key Laboratory of Biomembrane and Membrane Biotechnology, Tsinghua University, Beijing 100084, PR China

#### ARTICLE INFO

Article history: Received 15 April 2009 Available online 3 May 2009

Keywords:
Trichosanthin
Ribosome-inactivating protein
Plant toxin
HIV-1
Virus-like particles
Sorting strategy
Viral budding
Lipid raft
Anti-viral activity

#### ABSTRACT

Trichosanthin (TCS) is a type I ribosome-inactivating protein that plays dual role of plant toxin and antiviral peptide. The sorting mechanism of such an exogenous protein is in long pursuit. Here, we examined TCS trafficking in cells expressing the HIV-1 scaffold protein Gag, and we found that TCS preferentially targets the Gag budding sites at plasma membrane or late endosomes depending on cell types. Lipid raft membrane but not the Gag protein mediates the association of TCS with viral components. After Gag budding, TCS is then released in association with the virus-like particles to generate TCS-enriched virions. The resulting TCS-enriched HIV-1 exhibits severely impaired infectivity. Overall, the observations indicate the existence of a unique and elaborate sorting strategy for hijacking HIV-1.

© 2009 Elsevier Inc. All rights reserved.

## Introduction

Trichosanthin (TCS) is a 27-kDa protein extracted from the root tuber of *Trichosanthes kirilowii* [1]. TCS is a type I ribosome-inactivating protein (RIP), consisting of only a single polypeptide chain, which depurinates A-4324 of mammalian 28S rRNA via an *N*-glycosidase domain, thus arresting protein synthesis [2]. The protein has multiple documented functions, including abortifacient, antitumor, anti-HIV and immunoregulatory effects [3].

McGrath et al. [4,5] first described the anti-viral effects of TCS against HIV. TCS inhibited HIV replication in chronically infected H9 cells, an acutely infected T lymphoblastoid VB cell line, and primary macrophages chronically infected either *in vitro* or *in vivo* [4,5]. Phase I and II clinical trials conducted in US to evaluate the safety and potential efficacy of this drug have found that TCS elicits a moderate increase in circulating CD4<sup>+</sup> T cells and a significant decrease in p24 levels in AIDS patients failing treatment with antiretroviral agents such as zidovudine [6,7]. In addition to TCS, many other RIPs, including *Momordica* anti-HIV protein (MAP30), pokeweed anti-viral protein (PAP), and *Gelonium* anti-HIV protein (GAP31), have also been reported to inhibit HIV-1 replication *in vitro* [8].

The sorting pathway of TCS was under several investigations. TCS is efficiently endocytosed into late endosomes [3,9]. It was also reported that TCS is transported through exosome-mediated pathway [10]. As TCS is an anti-viral toxin, the sorting mechanism of TCS in HIV-1-infected cells is herein investigated and considered to be critical for understanding the anti-viral activity [8]. Interestingly, the budding virus apparently altered the sorting behavior of TCS. A significant fraction of TCS shows preferential targeting to viral components with the help of lipid rafts and the resulting TCS-enriched virions exhibit impaired infectivity. The data indicate the existence of a unique and powerful sorting strategy by TCS to hijack HIV-1.

# Materials and methods

Reagents and antibodies. Anti-actin, anti-rab5, anti-lamp1, antitsg101, anti-flotillin-1 and anti-transferrin receptor antibodies were from Santa Cruz Biotechnology. Anti-HIV-1 p24 antibody was from Biodesign International. Anti-TCS polyclonal antibody was prepared as standard protocol. Horseradish peroxidase labeled and fluorescently labeled secondary antibodies were from Zhong Shan Biotechnology. Methyl- $\beta$ -cyclodextrin (M $\beta$ CD) was from Sigma–Aldrich. The plasmid of Rev-independent Gag-GFP was a kind gift from Marilyn D. Resh (Memorial Sloan-Kettering Cancer Center, USA). Gag was subcloned to pcDNA3.1-Gag (Invitrogen) and pGag-CFP (Clontech) for expression.

<sup>\*</sup> Corresponding author. Fax: +86 10 6279 3367. E-mail address: suisf@mail.tsinghua.edu.cn (S.-F. Sui).

Cell culture and transfection. JAR, K562, U937 and MT4 cells were maintained in RPMI1640 (Gibco-BRL) supplemented 10% fetal bovine serum. JAR cell was transfected by lipofectamine2000 (Invitrogen) according to the manufacturer's protocol. Suspended cells as K562, MT4 and U937 cells were grown to  $2\times 10^7\, cells\, ml^{-1},$  resuspended in 10 mM Hepes-NaOH buffered PBS, mixed with 20  $\mu g$  plasmids, and further electroporated by BTX ECM 630 at 300 V for 20 ms.

Protein purification and labeling. TCS was extracted from the root tubers of *T. kirilowii* as described [10]. Fluorescent TCS was prepared by incubating the protein with fluorescein isothiocyanate (FITC) at a molar ratio of 1:5 (Protein: FITC) in 0.1 M Na<sub>2</sub>CO<sub>3</sub>–NaH-CO<sub>3</sub> buffer (pH 9.5). Unbound dyes were removed by extensive PBS dialysis after labeling.

Fluorescence microscopy. Transfected cells were grown on polyL-lysine coated glass coverslips. They were treated with 0.1  $\mu$ M FITC–TCS for 2 h. After incubation, the cells were washed extensively by PBS and fixed with 4% paraformaldehyde at 4 °C overnight. Samples were visualized by Nikon E800 microscope using a Plan-Apochromat oil 100  $\times$  1.4 numerical aperture objective. Digital images were acquired with SPOT-RT cold CCD camera (Diagnostic Instruments) driven and treated by the SPOT 3.5 software (Diagnostic Instruments). Color balance of Gag-CFP fluorescence was changed from blue to red for a better illustration.

Preparation of VLPs and HIV-1. JAR cells were fed with fresh medium at 24 h post-transfection of HIV-1 Gag. After next 24 h, the culture medium was collected, clarified continuously at 1000g for 20 min, 10,000g for 30 min to remove cell debris, and further filtered through a 0.22  $\mu$ M filter (Millipore). The filtrate was subjected to ultra filtration process by 100-kDa MWCO AmiconUltra (Millipore) and washed by extensive PBS to remove free proteins. They were then layered onto the top of a 20% (wt/vol) sucrose cushion in PBS and centrifuged for 2 h at 145,000g (P40ST rotor, Hitachi). VLPs were recovered from the bottom of the tube. For isolation of TCS-enriched VLPs, the transfected JAR cells were labeled with 0.1  $\mu$ M TCS for 4 h, then fresh culture medium was added for another 4 h. TCS-enriched VLPs were prepared as described above.

For preparation of HIV-1, MT4 cells ( $5 \times 10^4 \, \mathrm{ml}^{-1}$ ) were infected with HIV-1<sub>IIIB</sub> stock at a multiplicity of infection (MOI) of 0.1. After 3 days, 0.1  $\mu$ M TCS was incubated for 24 h. Then the medium was collected and the TCS-enriched virions were purified as above VLPs did. The quantity of virus was determined by HIV-1 p24 Antigen ELISA Kits (Vironostika) according to the manufacturer's protocol.

Sucrose density gradient and OptiPrep velocity gradient centrifugation. Once the culture supernatants were filtered through a 20% sucrose cushion, they were resuspended in 200 µL PBS and centrifuged in either sucrose equilibrium gradient or OptiPrep (60% w/v iodixanol, Axis-shieldy) velocity gradient as described [11].

Analysis for raft association. VLP membrane was prepared by 0.1% Triton X-100 treatment of VLP for 10 min and ultracentrifuged at 120,000g for 2 h. The pellets were collected as VLP membrane. VLP membrane was extracted by 0.5% Brji98 at 37 °C for 5 min and further analyzed by OptiPrep equilibrium flotation centrifugation as described [12]. The cholesterol from each fraction was measured with an Amplex Red cholesterol kit (Molecular Probes).

Bioassay for anti-HIV-1 activity. To determine the viral infectivity,  $5 \times 10^4 \, \text{ml}^{-1}$  MT4 cells were infected with equal amounts of HIV-1 for 2 h (MOI of TCS-free virus was 0.015). After washed off the unbounded virus, infected cells were placed in fresh culture medium for 3 days. The viral infectivity was assayed by produced p24 amount in culture medium by HIV-1 p24 Antigen ELISA Kits (Vironostika).

#### Results

TCS targets HIV-1 Gag budding regions at plasma membrane or late endosomes

Previous studies indicated that TCS alone is efficiently endocytosed into late endosomes [9,10]. To study TCS trafficking in HIV-1-infected cells, we used plasmids expressing the Rev-independent HIV-1 Gag scaffold protein, which is sufficient to produce virus-like particles (VLPs) and faithfully mimics the viral assembly and budding process [13]. We first expressed cyan fluorescent proteintagged Gag (Gag-CFP) in K562 and JAR cells, both of which are frequently used in studies investigating TCS. When fluorescein isothiocvanate (FITC)-labeled TCS was added to K562 cells, most of them were found internalized into the Gag-enriched intracellular compartments, although some were still at cell surface (Fig. 1). In the TCS-treated K562 cells, HIV-1 Gag localized predominantly to compartments containing endogenous Lamp1 and Tsg101, which define late endosomes, but not Rab5 (Supplemental Fig. 1). This is consistent with the previous study, which reported that HIV-1 mainly budded from late endosomes in K562 cells [13]. In JAR cells, considerable TCS was also enriched at the Gag budding sites, however, mainly on plasma membrane (Fig. 1). Because CD4<sup>+</sup> T cells and macrophages are natural hosts of HIV-1, we then examined FITC-TCS trafficking in human T-lymphocyte MT4 cells and human monocytic U937 cells. Although vast amounts of TCS were internalized into intracellular compartments, still considerable was accumulated at the Gag budding sites at cell periphery

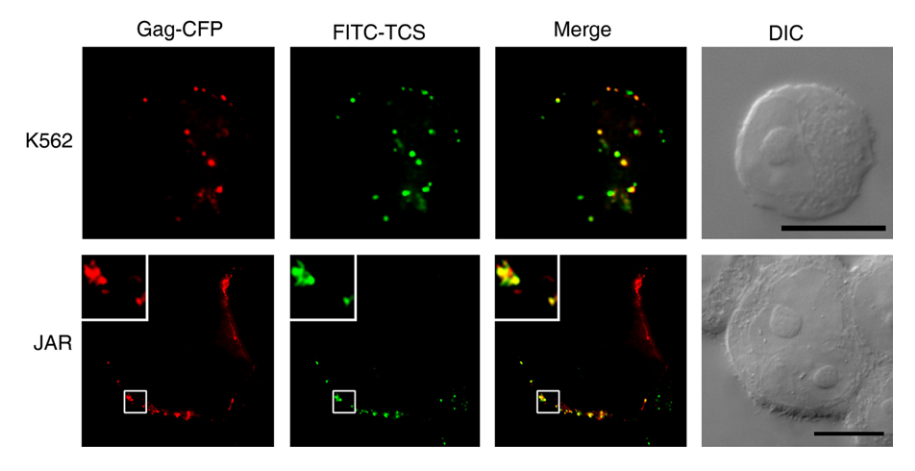


Fig. 1. TCS targets HIV-1 Gag budding regions. K562 and JAR cells expressing Gag-CFP were incubated with 0.1 μM FITC-TCS for 2 h. After washing and fixation, the cells were analyzed by fluorescence microscopy. Insets show a higher magnification of the boxed region. Central sections of cell are shown. Bar, 10 μm.

(Supplemental Fig. 2). Overall, the results indicate that TCS targets HIV-1 Gag budding sites at plasma membrane or late endosomes in various cell types.

# TCS is released in association with VLPs

As shown above, TCS was concentrated at HIV-1 Gag budding sites. After the budding of VLPs, TCS may be released into extracellular space with viral particles. VLPs can be captured, bound to poly-L-lysine coated glass coverslips, and visualized by fluorescence microscopy [14]. We then examined the cell-coverslip interface to detect the sign of secretion. TCS was clearly accumulated at the Gag-enriched extracellular puncta, which presumably represent VLPs (Fig. 2A). Moreover, after purification of VLPs from the above cells, TCS was also observed in fine association with the purified VLPs (Fig. 2B). Interestingly, the fluorescent spots within the cell, which we assumed to be VLPs or budding intermediates, were lacking in TCS (Fig. 2A). It is possible that the tight adherence of the cell to the coverslip prevented TCS from reaching these locations.

To provide further evidence that TCS associates with the VLPs, we examined its localization with respect to VLPs on a 20–60% linear sucrose density gradient. HIV-1 Gag and TCS were co-purified in exactly the same fractions (Fig. 2C). However, cell membrane microvesicles have a similar density to virions; as such, they can contaminate HIV-1 VLPs purified via linear sucrose density gradients. To eliminate this possibility, we used velocity sedimentation with a 6–18% OptiPrep gradient to separate VLPs from contaminating microvesicles. It is a well-accepted and high-purity method for purification of virions [11]. Once again, both TCS and Gag co-sedimented in the same bottom fractions (Fig. 2D).

We next determined the quantity of TCS that was released with VLPs versus that was retained in cells. It was shown that 51.6% of TCS was secreted with VLPs, and meanwhile 48.4% was present in cells (Fig. 2E). In the mock-treated control, only 8.3% of TCS was secreted. The data indicates that the sorting of TCS is changed to a great extent by the budding virus.

# TCS recognizes raft domain of VLP membrane

Immature VLPs are composed of both viral envelope and Gag shell. The viral membrane can be removed by nonionic detergent to generate the delipidized VLPs that hold a stable and intact Gag shell [15]. We measured the association of TCS with the normal or delipidized VLPs. Different from the Gag-interacting protein actin [16], TCS was found only associated with the normal VLPs but not the delipidized ones, which revealed the importance of viral membrane in the association (Fig. 3A).

Viral membrane is rich in lipid rafts with a high content of cholesterol and sphingolipids [17]. We further examined whether TCS specifically recognized the raft regions of VLP membrane. Although Triton X-100 is widely used for lipid rafts studies, Brji98 was found more appropriate for the rafts analysis on VLPs [12]. When VLP membrane was extracted by 0.5% Brji98, TCS was shown localized within the narrow raft fractions (defined by the specific distributions of Gag and cholesterol) (Fig. 3B and C).

HIV-1 Gag can efficiently recruit and cluster lipid rafts for the purposes of viral assembly and budding [18,19]. This may account for the sorting of TCS to viral particles. M $\beta$ CD is an effective cholesterol extractor and thus disrupts lipid rafts. After treating cells with M $\beta$ CD, TCS was redistributed from detergent-insoluble fractions to

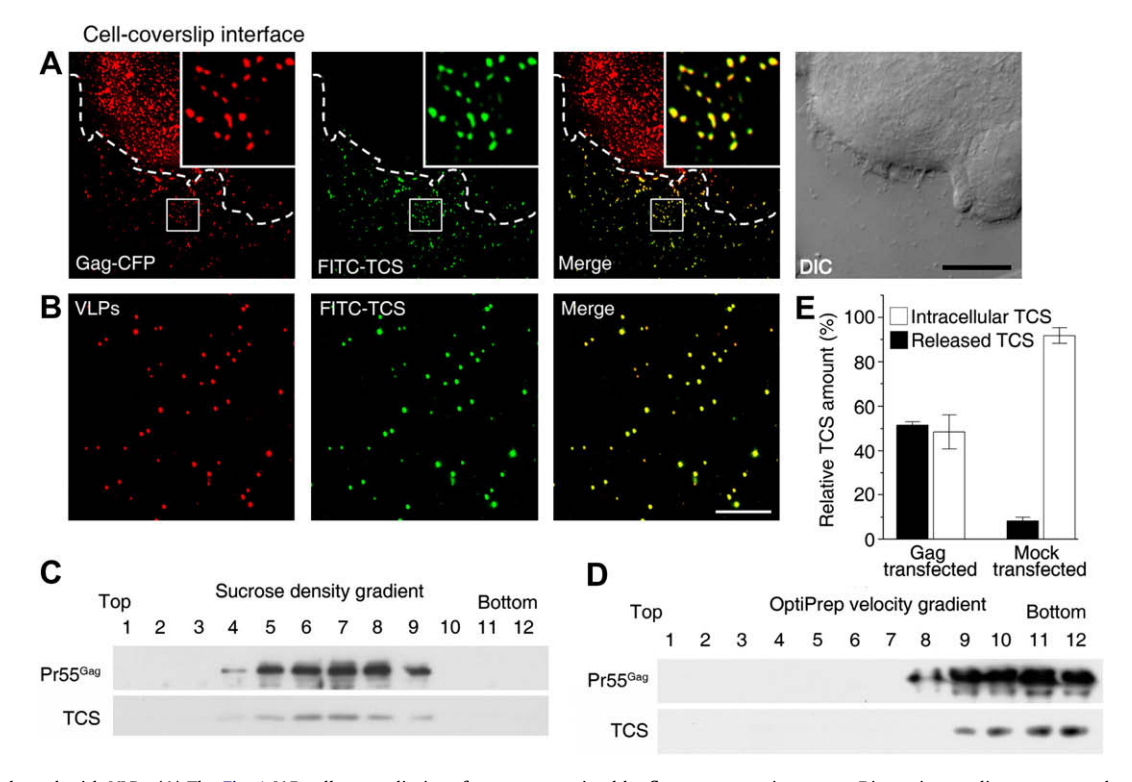


**Fig. 2.** TCS is released with VLPs. (A) The Fig. 1 JAR cell-coverslip interface was examined by fluorescence microscopy. Discontinuous lines separate the cell area and the extracellular milieu. Insets show a higher magnification of the boxed region. Bar, 10 μm. (B) FITC-TCS-enriched VLPs produced by the above JAR cells were purified and then loaded onto poly-t-lysine coated coverslip for fluorescence microscopy. Bar, 5 μm. (C) TCS-enriched VLPs were layered onto one of two gradients: 20–60% linear sucrose gradient accelerated to equilibrium (16 h at 200,000g) to monitor particle density, or (D) 6–18% linear OptiPrep gradient accelerated to a shorter duration (1.5 h at 250,000g) to monitor velocity of particle sedimentation. Fractions (12) were collected from the top to the bottom and analyzed by Western blotting. (E) JAR cells were first incubated with 0.1 μM FITC-TCS for 2 h, washed and further cultured in fresh medium for 1 h. The quantity of TCS in association with cells or VLPs was measured by fluorescence spectrophotometer (at 495-nm excitation). For the mock-treated control, TCS recruited by possible microvesicles was collected by an ultracentrifugation of 120,000g for 2 h. The released TCS (black bar) and intracellular TCS (white bar) together make up a total amount of 100% (±SEM; *n* = 3).

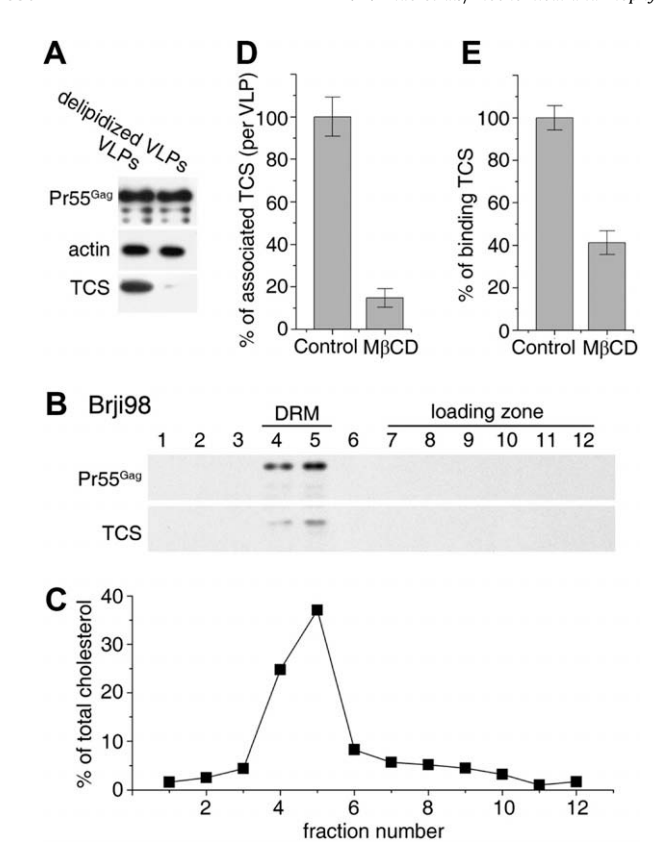


Fig. 3. TCS recognizes the lipid raft region of VLP membrane. (A) TCS fails to associate with the delipidized VLPs. To remove the lipid bilayer of TCS-enriched VLPs, they were treated with 0.5% Triton X-100 at 37 °C for 30 min. The denuded Gag shell of immature VLPs and mock-treated VLPs were pelleted by ultracentrifugation and analyzed by Western blotting. (B) VLP membrane was extracted with 0.5% Brii98 at 37 °C for 5 min and then subjected to OptiPrep equilibrium flotation centrifugation consisting of a 56% loading zone overlaid with 30%, 25%, and 5% OptiPrep solutions. Pr55<sup>Gag</sup> and TCS from each fraction were detected by Western blotting. DRM indicates detergent-resistant membrane. (C) Cholesterol profile of the rafts analysis in panel B. (D) Effect of rafts disruption on TCS sorting to VLPs. JAR cells expressing Gag were incubated with 0.1  $\mu M$  FITC–TCS and treated with 10 mM MβCD for 1 h. After wash with PBS, fresh non-serum medium was then added for 2 h. Equal amounts of the released VLPs were used for quantification of the associated FITC-TCS by fluorescence spectrophotometer. The data is shown as percentage of FITC-TCS fluorescence in untreated control ( $\pm$ SEM, n=3), (E) Effect of rafts disruption on in vitro binding of TCS to VLPs. Purified VLPs were first pretreated with 10 mM M<sub>B</sub>CD for 1 h and then incubated with 0.5  $\mu$ M FITC-TCS for 2 h. After ultracentrifugation and wash with a large volume of PBS, the pellets were resuspended and FITC-TCS was measured by fluorescence spectrophotometer. The data is shown as percentage of FITC-TCS fluorescence in untreated control (±SEM, n = 3).

detergent-soluble fractions (Supplemental Fig. S3). The amount of associated TCS per VLP was significantly down-regulated (Fig. 3D). Meanwhile, the production of VLPs was reduced to a less extent as previous report (data not shown) [19]. To gain direct evidence of the interaction between TCS and lipid rafts, we performed an *in vitro* binding assay. The binding of TCS to VLPs was largely diminished after pretreatment with M $\beta$ CD (Fig. 3E). Because TCS and Gag are originally from opposite faces of the membrane, we deduce that lipid rafts but not Gag protein contribute majorly to the recruitment of TCS to viral components.

# TCS-enriched HIV-1 exhibits impaired infectivity

After demonstrating that TCS associates with viral particles, we then examined whether these TCS-enriched HIV-1 show reduced infectivity. Equal amounts of TCS-enriched or mock control HIV-1 were used to infect fresh MT4 cells. The amount of p24 released

into the culture medium was quantified as an indicator of infectivity as in previous studies [4,5]. TCS-enriched virions showed only  $\sim\!\!20\%$  infectivity compared to the control virus (Fig. 4). Such a prominent inhibition is likely due to the association of TCS with virus, for an equivalent amount of free TCS showed a very minor inhibitory effect. Thus, the TCS enriched in HIV-1 potently inhibits viral infectivity.

#### Discussion

We reported here a novel sorting pathway of the anti-viral toxin of TCS. Exogenous TCS is taken up by HIV-1-infected cells and associated with the lipid rafts on HIV-1 budding sites, where the TCSenriched virions were generated. The selective association of TCS with viral components severely impairs the viral infectivity, which hints of a direct effect of TCS on HIV-1 virions. TCS exploits the sorting strategy to eradicate both the budding and cell-free virus, and potentially prevents the virus dissemination. The trafficking pathway of TCS also contributes to explain its virus eradication effects on HIV-1 that buds from plasma membrane or more importantly in the hidden reservoir of late endosomes [4]. However, in response to the hijacking, virus may develop an effective escaping strategy. HIV-1 tends to bud at the tight cell-cell contact of virological synapse to prevent exogenous attacking [20]. Here, we observed that TCS was unable to hijack the VLPs at the tight cell-cell contact or cell-coverslip contact (Figs. 1 and 2A).

TCS recognizes HIV-1 through viral envelope. The viral envelope is rich in lipid rafts with a high content of cholesterol and sphingolipid, which is strikingly different from host cell membrane [17]. The budding HIV-1 recruits sufficient raft membranes and thus incorporates some raftophilic proteins in spite of the low concentration on plasma membrane, at the same time excludes the abundant non-raft proteins such as CD45 [18]. Therefore, it is an elaborated strategy for the protein-based drug to hijack the lipid rafts of viral envelope.

TCS is a plant toxin with sequence homology to the ricin A chain [1]. At low doses, TCS shows anti-viral activity without significant toxicity, whereas high doses induce apoptosis, especially in HIV-1-infected cells [4,21]. TCS is normally transported into the interior of cell, and meanwhile HIV-1 buds outward into the extracellular space. When the two meet at plasma membrane or late endosomes, a significant fraction of TCS is recruited and carried by the budding virus for secretion, which changes the trafficking itin-

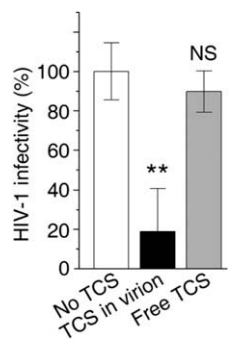


**Fig. 4.** TCS-enriched HIV-1 shows severely impaired infectivity. Equal amounts of the following HIV-1 (normalized for p24) were prepared to infect MT4 cells. (1) Mock-treated control HIV-1 (No TCS). (2) TCS-enriched HIV-1 ( $\sim$ 5 ng TCS for  $10^5$  cells) prepared as in materials and methods (TCS in virion). (3) Normal HIV-1, when infects cells, adding free TCS at the equivalent amount as the above TCS-enriched HIV-1 (free TCS). P24 antigen level in the supernatant was determined by capture ELISA as an indicator of infectivity. The values indicate percentages of p24 amount compared to that of the control virus (±SEM; n = 3). The data were analyzed using Student's t-test. "p < 0.01; NS, not significant (p > 0.05).

erary of the incoming TCS. Although it is not new for the virions to mediate the transport of pathogenic factors as prion protein PrPsc [22], our report is definitely the first to show the virion-mediated secretion of plant toxin.

In conclusion, the current study provides evidences on a novel sorting strategy of TCS for effective virus eradication. It extends the current understandings of the trafficking relationship between exogenous peptide and virus. Because TCS has a unique feature of specific association with HIV-1, it can provide new implications to develop the protein-based therapies for AIDS.

## Acknowledgments

We thank Dr. Jing-Yun Li for the help of HIV-1 work in Laboratory Biosafety Level-3 (Academy of Military Medical Sciences of China) and Marilyn D. Resh (Memorial Sloan-Kettering Cancer Center, USA) for Gag-GFP plasmid. This work was supported by National Natural Science Foundation of China and National Basic Research Program of China (2004CB720005).

# Appendix A. Supplementary data

Supplementary data associated with this article can be found, in the online version, at doi:10.1016/j.bbrc.2009.04.124.

#### References

- J.M. Maraganore, M. Joseph, M.C. Bailey, Purification and characterization of trichosanthin. Homology to the ricin A chain and implications as to mechanism of abortifacient activity, J. Biol. Chem. 262 (1987) 11628–11633.
- [2] J.S. Zhang, W.Y. Liu, The mechanism of action of trichosanthin on eukaryotic ribosomes – RNA N-glycosidase activity of the cytotoxin, Nucleic Acids Res. 20 (1992) 1271–1275.
- [3] P.C. Shaw, K.M. Lee, K.B. Wong, Recent advances in trichosanthin, a ribosome-inactivating protein with multiple pharmacological properties, Toxicon 45 (2005) 683–689.
- [4] M.S. McGrath, K.M. Hwang, S.E. Caldwell, I. Gaston, K.C. Luk, P. Wu, V.L. Ng, S. Crowe, J. Daniels, J. Marsh, et al., GLQ223: an inhibitor of human immunodeficiency virus replication in acutely and chronically infected cells of lymphocyte and mononuclear phagocyte lineage, Proc. Natl. Acad. Sci. USA 86 (1989) 2844–2848.

- [5] M.S. McGrath, S. Santulli, I. Gaston, Effects of GLQ223 on HIV replication in human monocyte/macrophages chronically infected in vitro with HIV, AIDS Res. Hum. Retroviruses 6 (1990) 1039–1043.
- [6] V.S. Byers, A.S. Levin, A. Malvino, L. Waites, R.A. Robins, R.W. Baldwin, A phase II study of effect of addition of trichosanthin to zidovudine in patients with HIV disease and failing antiretroviral agents, AIDS Res. Hum. Retroviruses 10 (1994) 413–420.
- [7] V.S. Byers, A.S. Levin, L.A. Waites, B.A. Starrett, R.A. Mayer, J.A. Clegg, M.R. Price, R.A. Robins, M. Delaney, R.W. Baldwin, A phase I/II study of trichosanthin treatment of HIV disease, AIDS 4 (1990) 1189–1196.
- [8] B.A. Parikh, N.E. Tumer, Antiviral activity of ribosome inactivating proteins in medicine, Mini Rev. Med. Chem. 4 (2004) 523–543.
- [9] W.Y. Chan, H. Huang, S.C. Tam, Receptor-mediated endocytosis of trichosanthin in choriocarcinoma cells, Toxicology 186 (2003) 191–203.
- [10] F. Zhang, S. Sun, D. Feng, W.L. Zhao, S.F. Sui, A novel strategy for the invasive toxin: hijacking exosome-mediated intercellular trafficking, Traffic 10 (2009) 411–424.
- [11] M. Dettenhofer, X.F. Yu, Highly purified human immunodeficiency virus type 1 reveals a virtual absence of Vif in virions, J. Virol. 73 (1999) 1460–1467.
- [12] K. Holm, K. Weclewicz, R. Hewson, M. Suomalainen, Human immunodeficiency virus type 1 assembly and lipid rafts: Pr55(gag) associates with membrane domains that are largely resistant to Brij98 but sensitive to Triton X-100, J. Virol. 77 (2003) 4805–4817.
- [13] S. Nydegger, M. Foti, A. Derdowski, P. Spearman, M. Thali, HIV-1 egress is gated through late endosomal membranes, Traffic 4 (2003) 902–910.
- [14] Y. Fang, N. Wu, X. Gan, W. Yan, J.C. Morrell, S.J. Gould, Higher-order oligomerization targets plasma membrane proteins and HIV gag to exosomes, PLoS Biol. 5 (2007) e158.
- [15] Y. Morikawa, M. Shibuya, T. Goto, K. Sano, In vitro processing of human immunodeficiency virus type 1 Gag virus-like particles, Virology 272 (2000) 366–374.
- [16] B. Liu, R. Dai, C.J. Tian, L. Dawson, R. Gorelick, X.F. Yu, Interaction of the human immunodeficiency virus type 1 nucleocapsid with actin, J. Virol. 73 (1999) 2901–2908.
- [17] B. Brugger, B. Glass, P. Haberkant, I. Leibrecht, F.T. Wieland, H.G. Krausslich, The HIV lipidome: a raft with an unusual composition, Proc. Natl. Acad. Sci. USA 103 (2006) 2641–2646.
- [18] D.H. Nguyen, J.E. Hildreth, Evidence for budding of human immunodeficiency virus type 1 selectively from glycolipid-enriched membrane lipid rafts, J. Virol. 74 (2000) 3264–3272.
- [19] A. Ono, E.O. Freed, Plasma membrane rafts play a critical role in HIV-1 assembly and release, Proc. Natl. Acad. Sci. USA 98 (2001) 13925–13930.
- [20] C. Jolly, Q.J. Sattentau, Retroviral spread by induction of virological synapses, Traffic 5 (2004) 643–650.
- [21] Y.Y. Wang, D.Y. Ouyang, H. Huang, H. Chan, S.C. Tam, Y.T. Zheng, Enhanced apoptotic action of trichosanthin in HIV-1 infected cells, Biochem. Biophys. Res. Commun. 331 (2005) 1075–1080.
- [22] P. Leblanc, S. Alais, I. Porto-Carreiro, S. Lehmann, J. Grassi, G. Raposo, J.L. Darlix, Retrovirus infection strongly enhances scrapie infectivity release in cell culture, EMBO J. 25 (2006) 2674–2685.